Automated road extraction from terrestrial based mobile laser scanning system using the GVF snake model

Conference Paper · November 2010

CITATIONS
12

READS
289

3 authors:

Pankaj Kumar
Centre Tecnològic de Telecomunicacions de Catalunya (CTTC), Barcelona, Spain
22 PUBLICATIONS **305** CITATIONS
SEE PROFILE

Timothy Mccarthy
National University of Ireland, Maynooth
43 PUBLICATIONS **549** CITATIONS
SEE PROFILE

Conor Mc Elhinney
National University of Ireland, Maynooth
53 PUBLICATIONS **639** CITATIONS
SEE PROFILE

Automated road extraction from terrestrial based mobile laser scanning system using the GVF snake model

Pankaj Kumar, Tim McCarthy, Conor P. McElhinney

National Centre for Geocomputation (NCG),
National University of Ireland Maynooth (NUIM),
Maynooth, Co. Kildare, Ireland
pankaj.kumar.2009@nuim.ie

KEY WORDS: road networks, mobile mapping system, LiDAR, point cloud, GVF snake

ABSTRACT:
Accurate extraction and reconstruction of route corridor features from geospatial data is a pre-requisite to effective management of road networks for engineering, safety and environmental applications. High quality road geometry and road side features can now be extracted from dense point cloud LiDAR data, recorded by modern day Mobile Mapping Systems. This valuable route network information is gaining the attention of road safety and maintenance engineers. Road points are needed to be correctly identified, classified and extracted from LiDAR data before reconstructing intrinsic road geometry and road-side infrastructure. In this paper, we present a method to automatically extract the road from terrestrial based mobile laser scanning system using the GVF (Gradient Vector Flow) snake model. A snake is an energy minimizing spline that moves towards the desired feature or object boundary under the influence of internal forces within the curve itself and external GVF forces derived typically from 2D imaging data by minimizing certain energy such as edges or high frequency information. In our novel method, we initialise the snake contours over point cloud data based on the trajectory information produced by the MMS navigation sub-system. The internal energy term provided to the snake contour is based on adjusting the intrinsic properties of the curve, such as elasticity and bending, whilst the GVF energy and constraint energy terms are derived from the LiDAR point cloud attributes. Our method primarily differs from the traditional snake models in initialisation and in deriving the energy terms from the 3D LiDAR data.

1. INTRODUCTION

Road transportation has a central role to play in the progress and socio-economical growth of European society by providing efficient mobility, in particular by minimizing time and effort in connecting human demand with the existing supply of products and services in society. The transport of goods between European member states is set to increase by 50 % between 2000 and 2020. The road transport sector itself already contributes hugely to the European economy as it provides about 4.5 million jobs and generates a turnover worth about 1.6 % of European Union (EU) Gross Domestic Product (GDP) with almost 293 million vehicles travelling over 5 million kilometres of road network (European Commission 2006). However, road accidents have become one of the main concerns for policy makers and road infrastructure developers due to the thousands of death and huge economic loss caused by them. In 2006, around 40,000 people lost their lives while 1.8 million people were injured in road accidents across EU (ERSO 2008). Road accidents are the leading cause of death and hospital admission for people younger than 50 years in EU. The socio-economic cost has been estimated at around 2% of EU countries GDP – around 180 billion Euro and twice the EU's annual budget (SafetyNet 2009).

The main cause of road accidents can be attributed to vehicle, driver-behaviour and road infrastructure or environment. A number of vehicle safety initiatives, such as the European New Car Assessment (Euro NCAP), deal with the safety aspects of road vehicles. Euro NCAP makes available to consumers independent information about a vehicle's comparative safety and acts as an incentive for manufacturers to improve the safety of their vehicles. Improvements in driver behaviour are covered by a number of initiatives including training and driver licensing.

Road infrastructure design has an effect on accident risk because it can determine how road users perceive their environment. Recent investigations have shown a strong relationship between road infrastructure and driver speed, acceleration and lateral position. These driver behaviour characteristics are known to be amongst the most important values in accident analysis (Gatti et al. 2007). Significant changes in geometric design standard elements and physical road factors tend to increase accident frequency and severity. Road infrastructure related safety measures offer the potential for reducing road accidents and their consequences. Several EU road safety audits and inspections exist which qualitatively estimate and report on potential road safety issues and identify opportunities for improvements in road infrastructure and design schemes. Current road inspection surveys are manual and involve an engineer annotating a digital map or using spatially referenced video to manually classify various features along the route (Eenink et al. 2008). The information collected through these surveys is sometimes incomplete and insufficient to support accurate diagnosis and intervention. It can also be time consuming and expensive to conduct these inspections on a large scale. A recent research call highlighted the requirement for common evaluation tools and implementation strategies in carrying out these inspections and assessing risks along route corridors (ERA-NET 2009).

Terrestrial based mobile mapping systems (MMSs) present a reliable, automated and cost effective alternative for road safety inspection. LiDAR point cloud data recorded by modern day MMSs can be employed to extract road features and reconstruct the route corridor in 3D. Laser scanning provide highly accurate and dense point cloud data from which detailed 3D models can be generated. Several attempts have been made to segment the road and its features from airborne as well as terrestrial based LiDAR data. (Clode et al. 2004) made use of a hierarchical classification technique to classify the airborne LiDAR intensity and range data into road and non-road objects. (Saeedi et al. 2009) described the potential of artificial swarm bee colony clustering algorithm for object extraction from LiDAR data. Some of the road segmentation approaches are based on fitting lines to the LiDAR data to search for a horizontal straight line (Yuan et al. 2008), using a Hough transformation to extract the road stripes from integrated LiDAR and high resolution imagery (Hu et al. 2004) and detecting curbstones from airborne laser scanning data (Vosselman & Liang 2009).

Active contour models, known as snakes (Kass et al. 1988), have also been utilized for segmenting road and urban features from airborne image and LiDAR datasets. (Kerschner 2001) developed a twin snake concept for detecting two parallel contours simultaneously from high resolution imagery. They extended the snake's energy function by an additional term formulating the attraction force to a curve parallel to its twin partner. (Kabolizade et al. 2010) proposed an improved snake model that focuses on building extraction from colour aerial images and LiDAR data. The model was modified in the external energy function and in a selection of initial seed contour from the NDSM (Normalized digital surface model) data set. (Goepfert & Rottensteiner 2009) applied an active contour approach to the airborne laser scanning data for extracting the 2D road networks. In their approach, the contour was initialized with the vector data while the image energy was derived from the laser data to extract the road features which were later used to match two datasets.

However, the majority of the road segmentation algorithms only intend to find the location of the road but does not make any attempt to extract the edges, border or surface of the road. In order to obtain accurate information about the road geometry and its features, we first need to extract road edges from the LiDAR data and subsequently the road points in between them. In this paper, we present a method to automatically extract the road edges from terrestrial based MMS using the GVF (Gradient Vector Flow) snake model. In section 2, we give a general overview of MMSs and describe our own Experimental Platform (XP-1) system. In section 3, the traditional and the GVF snake model are discussed. The implementation of the GVF snake model on LiDAR data is described in section 4. In section 5, the experimental results from implementing the snake model are presented and finally, we have drawn conclusions in section 6.

2. MOBILE MAPPING SYSTEM (XP-1)

With the potential of Geographical Information System (GIS) technologies in applications such as route corridor surveying, road signs inventory, cadastral surveys, traffic and urban planning, there has been a corresponding development in terrestrial based Mobile Mapping technologies. Mobile Mapping refers to a means of collecting geospatial data using mapping and navigation sensors that are rigidly mounted together on a mobile platform (Tao & Li 2007). The effectiveness of Mobile Mapping lies in its ability to directly georeference the mapping sensors relative to the navigation sensor. The spatially-referenced data obtained from Mobile Mapping is more dense, rapid and less expensive when compared to the more conventional methods.

The first terrestrial based MMS was developed in the 1980s by the Ohio State University for highway inventories (Novak 1993). Their system integrated GPS and gyro based inertial system alongside digital stereo vision and colour video cameras. Due to the wide range of MMS applications, it has now developed from a topic of academic interest to a commercially viable industry. There are number of companies which provide Mobile Mapping services to the user community for fast and automated data acquisition (Kingston et al. 2007) (Hunter et al. 2006). We have recently completed design and development of a terrestrial based MMS, experimental platform (XP-1), at NUI Maynooth as shown in Fig.1.

Figure 1: XP 1 Mobile Mapping System.

Our MMS comprises of an IXSEA LandINS GPS/INS, a Riegl VQ-250 300 KHz laser scanner and imaging system consisting of 6 progressive scanner cameras (1280*1024), FLIR thermal (un-cooled) SC-660 camera and an innovative 5-CCD multispectral camera capable of sensing across visible and infrared bandwidths. At the heart of the LandINS is a high grade, solid-state fibre optic gyroscope (FOG) technology with a drift rate of better than 0.05/hr. A distance measuring instrument (DMI), which is fitted to the wheel of the vehicle captures movement over the ground and is used in computing the final navigation solution during post-processing. The specifications for the Riegl VQ-250 LiDAR are shown in Table 1. The LiDAR system is mounted on the back of the van at a 45^0 angle from both the horizontal and vertical axis of the vehicle. It captures up to 1 million points every 3.5 seconds using a 300 kHz sensor which leads to approximately 20 GB of data per hour.

Measurement Rate	300kHz
Minimum Range (m)	1.5
Accuracy (m)	0.01
Precision (m)	0.01
Intensity	16 bit
Field of view (deg)	360
Angular Resolution (deg)	0.001

Table 1: Riegl VQ-250 specifications.

3. ACTIVE CONTOUR (SNAKE) MODEL

The concept of snakes or active contours was first introduced by (Kass et al. 1988) and since then, it has been widely accepted in computer vision and pattern recognition systems. Active contours are used in many applications including edge detection, image segmentation, object boundary localisation, shape modelling, motion tracking, medical image analysis, stereo matching and 3D reconstruction. Active contours are controlled splines defined within an image domain that moves towards the desired feature or object boundary under the influence of internal forces within the curve itself and external forces derived from the image data. The contour is defined in the (x, y) plane of an image as a parametric curve $v(s) = (x(s), y(s))$, where s is the normalized arc length. The contour $v(s)$ is represented by a set of control points $v_0, v_1 \ldots\ldots\ldots v_{n-1}$ and the curve is linearly obtained by joining each control point. In the traditional snake model, the behaviours of the snake are governed by the energy function which is defined as

$$E_{snake} = \int_0^1 (E_{\text{int}}(v(s)) + E_{ext}(v(s)))ds \qquad (1)$$

where E_{int} and E_{ext} are the internal energy and external energy term. The internal energy function E_{int} depends on the intrinsic properties of the curve and can be written as

$$E_{\text{int}} = \frac{1}{2}((\alpha(s)\left|v'(s)\right|^2 + \beta(s)\left|v''(s)\right|^2) \qquad (2)$$

where α and β are weight parameters, $v'(s)$ is first derivative of $v(s)$ with respect to s and $v''(s)$ is second derivative of $v(s)$ with respect to s. The internal energy equation (2) is composed of a first-order term designed to hold the curve together (discourage stretching) and a second-order term designed to keep the curve from bending too much (discourage bending). The weighting parameter α is a measure of the elasticity in the snake and controls the tension while β is a measure of stiffness in snake and controls the rigidity.

The external energy function E_{ext} is derived from the edge function that attracts the snake towards the desired image edges with high gradient value. It can be described as

$$E_{ext} = -\gamma\left|\nabla I(v(s))\right|^2 \qquad (3)$$

where γ is external energy weight parameter, ∇ is gradient operator and $I(v(s))$ is greyscale image. In order to make the snake model converge to the desired image object, the snake energy function E_{snake} should be minimized with

$$\alpha v''(s) - \beta v'''(s) - \nabla E_{ext} = 0. \qquad (4)$$

However, the traditional snake or active contour model is associated with two limitations in contour detection (Xu & Prince 1998). First, the initial contour must be close to the true boundary or else it will converge to the wrong result i.e. small capture range. Secondly, active contour fails to detect concave boundaries. Various methods have been proposed to overcome the initialization and concavity issue of the snake active contours. (Cohen 1991) introduced balloon forces to the active contour model. (Amini et al. 1990) used dynamic programming to minimize the energy of active contours. (Leroy et al. 1996) used a multi-resolution concept in active contour model. However, most of the proposed methods solved only one problem but creating new complexities. (Xu & Prince 1998) suggested a new external force field for active contour models called GVF (gradient vector flow). The GVF snake model can achieve better results due to its insensitivity to initialization and its ability to converge to concave boundaries. GVF fields are dense vector fields which are computed as a diffusion of the gradient vectors of a gray level or binary edge map derived from the image.

In the GVF model, the vector field is defined as $V(x,y) = (u(x,y), v(x,y))$, which minimizes the energy function

$$\varepsilon = \int\int \mu(u_x^2 + u_y^2 + v_x^2 + v_y^2) + \left|\nabla f\right|^2 \left|V - \nabla f\right|^2 dxdy \qquad (5)$$

where u and v are the vector components of GVF field V, μ is the regularization parameter that is set according to the amount of noise present in the image and f represents an edge map. The GVF field can be found by treating u and v as functions of time t and solving the following Euler equations

$$u_t(x,y,t) = \mu\nabla^2 u(x,y,t) - (u(x,y,t) - f_x(x,y)).(f_x(x,y)^2 + f_y(x,y)^2) \qquad (6a)$$

$$v_t(x,y,t) = \mu\nabla^2 v(x,y,t) - (v(x,y,t) - f_y(x,y)).(f_x(x,y)^2 + f_y(x,y)^2) \qquad (6b)$$

where ∇^2 is Laplacian operator. After computing $V(x,y)$, the external force $-\nabla E_{ext}$ in equation (4) is replaced by

$$v_t(s,t) = \alpha v''(s,t) - \beta v''''(s,t) + V\,. \qquad (7)$$

Thus the parametric curve that solves the above dynamic equation is called a GVF snake and is solved with an iterative solution (Xu & Prince 1998). In the next section, we demonstrate the implementation of GVF snake model on LiDAR data.

4. GVF SNAKE MODEL IMPLEMENTATION

The GVF snake model is implemented by deriving its energy terms from the LiDAR point data and then initialising the snake contour based on the navigation information. The behaviour of the snake is governed by three energy terms i.e. internal, GVF and external constraint energy. The internal energy input is based on adjusting the intrinsic properties i.e. elasticity and bending of the curve. The GVF energy is computed by diffusing the gradient vectors of edge function derived from the surface slope of LiDAR data while the external constraint energy is derived from the edge function gradient of LiDAR intensity values which contain the reflectance properties of the objects. The values for internal energy, E_{int}, are qualitatively determined by modifying the elasticity and rigidity terms.

In order to calculate the GVF energy from the surface slope, we first need the digital terrain model (DTM) of the LiDAR point data. However, a general problem associated with LiDAR point cloud is the high frequency noise present due to low vertical accuracy relative to horizontal sample distance which can lead to a poor quality DTM. This noise can be reduced via a point thinning and smoothing process by building the DTM pyramid. A DTM pyramid is composed of a list of pyramid layers, with the first layer corresponds to the full resolution DTM and the last layer corresponds to the DTM of lowest resolution. Point thinning over LiDAR points is achieved using the z-mean window filter method which thins points for each pyramid level by partitioning the data into equal areas (windows) and then one or two points closest to the mean z-value are selected from each area. The window size is kept equal to the average point spacing in the LiDAR point cloud data. After building the DTM surface, the slope is calculated as the rate of change of the surface in the horizontal (dz/dx) and vertical (dz/dy) directions from its centre point to its neighbours by the natural neighbourhood interpolation method. Finally, the GVF energy, E_{GVF}, is determined by diffusing the gradient vectors of the edge function from the slope surface. The external constraint energy, E_{const}, of the snake contour is estimated from the edge function gradient of the intensity values of the LiDAR echoes. Thus, the properties of both the LiDAR attributes are exploited to generate the energy terms for the snake contour.

$$E_{snake} = E_{\text{int}} + \kappa \times E_{GVF} + \lambda \times E_{const} \qquad (8)$$

where κ, λ are the weight parameters that can be adjusted by the user's emphasis.

We initialise the snake contour over LiDAR point cloud data based on the trajectory information produced by the MMS navigation system along the road sections. The dimensions of the LiDAR data are provided as an input to the algorithm which allows us to choose an ellipse

contour for initialising the snake. The snake points are initialised in the form of a parametric ellipse (as shown in Fig. 2) which can be expressed as

$$X(t) = X_C + a\cos(t)\cos(\phi) - b\sin(t)\sin(\phi) \quad (9a)$$

$$Y(t) = Y_C + a\cos(t)\sin(\phi) + b\sin(t)\cos(\phi) \quad (9b)$$

where t varies from 0 to 2π, ϕ is the angle between the X-axis and major axis of the ellipse and X_C, Y_C are the centre of the ellipse.

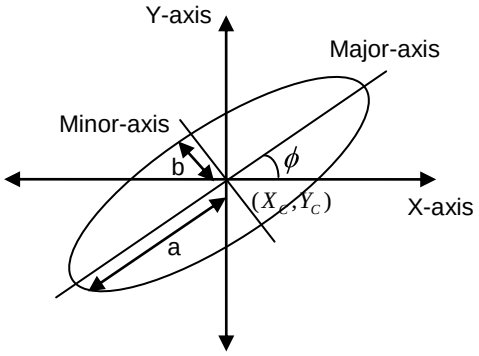

Figure 2: Snake Contour Initialization in Parametric Ellipse Form.

The major axis of the initial snake ellipse was computed from the middle and first navigation point while the difference between middle navigation point and the estimated centre of the road point was taken as minor axis. The average heading information of the vehicle was used for providing the direction to the snake contour i.e. ϕ value. The experimental results from implementing the GVF snake model over LiDAR point cloud datasets are presented in next section.

5. EXPERIMENTAL ANALYSIS

The snake algorithm was tested over LiDAR points from two different road sections with each covering an area of width 30 m and length 10 m as shown in Fig. 3 and 4. In our first road section, the snake contour was initialised based on the navigation points with an average heading information of 63.64^0 (with respect to north direction) as shown in Fig.5 (a) (with first and middle navigation points represented as yellow dots over the 2D road surface). After examining several combinations of weight parameters, we provided α =4.6, β =0.001, γ =4, κ =4.5, λ =1.5 and no. of iterations = 30 to the snake contour (Fig.5 (b)). After reaching the minimum energy state, the snake contour converged to the road edges as shown in Fig.5 (c).

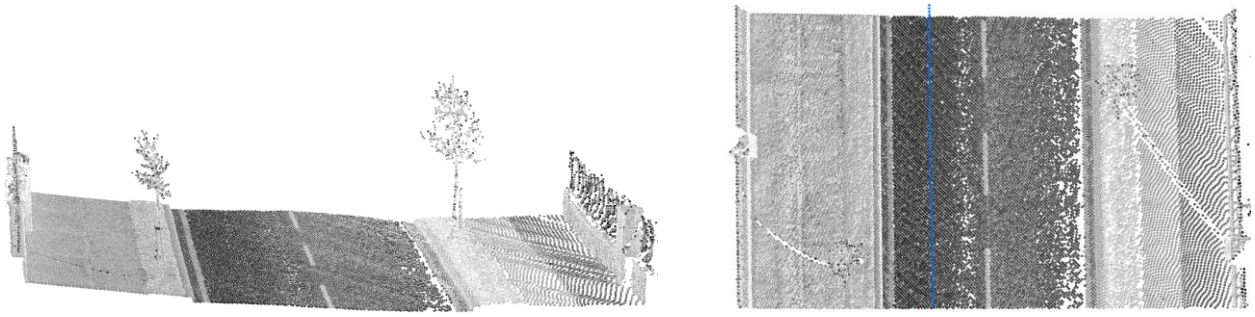

(a) **(b)**

Figure 3: (a) Planar view of LiDAR point data of first road section (b) Bird's eye view of LiDAR point along with Navigational point data (blue dots) of first road section.

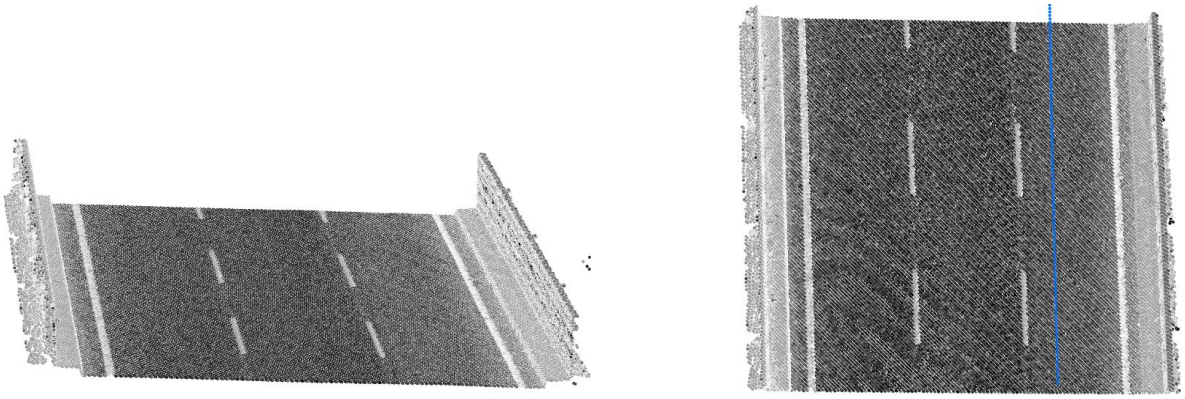

(a) (b)

Figure 4: (a) Planar view of LiDAR point data of second road section (b) Bird's eye view of LiDAR point along with Navigational point data (blue dots) of second road section.

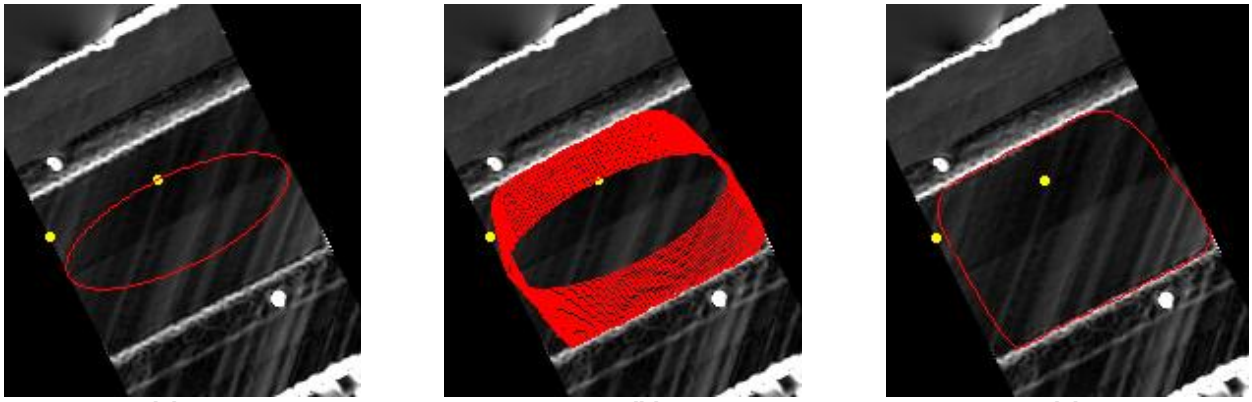

(a) (b) (c)

Figure 5: (a) Snake contour initialization based on navigation information over first test section of 2D road surface (b) Snake Contour during iterative process (c) Output snake contour.

In the second road section, the navigation points had an average heading of 110.82^0 (with respect to north direction) which was utilised to initialise the snake contour as shown in Fig.6 (a). The parameters provided to the snake contour were α =0.7, β =0.001, γ =3, κ =5.8, λ =0.5 and no. of iterations = 30 (Fig.6 (b)). The final snake contour is shown in Fig.6 (c).

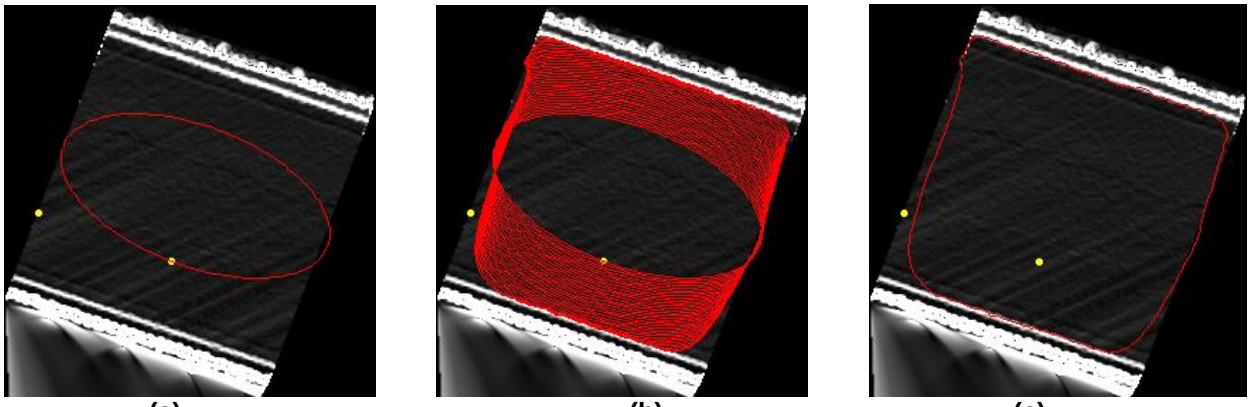

(a) (b) (c)

Figure 6: (a) Snake contour initialization based on navigation information over second test section of 2D road surface (b) Snake Contour during iterative process (c) Output snake contour.

The results of the road edge detection from the snake model for the two road sections has been represented over the 3D LiDAR point cloud data in Fig. 7 and 8.

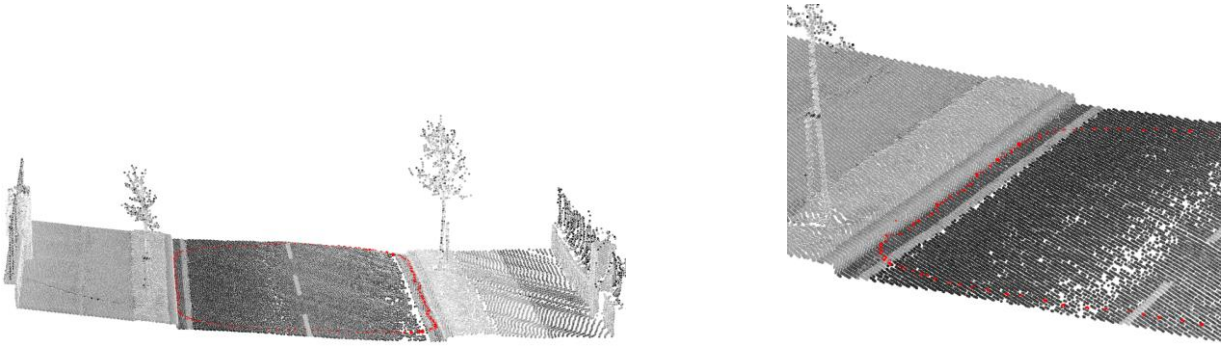

(a) (b)

Figure 7: (a) Planar view of estimated road edges over first road section highlighted in red colour (b) zoomed-in estimated road edges over first road section.

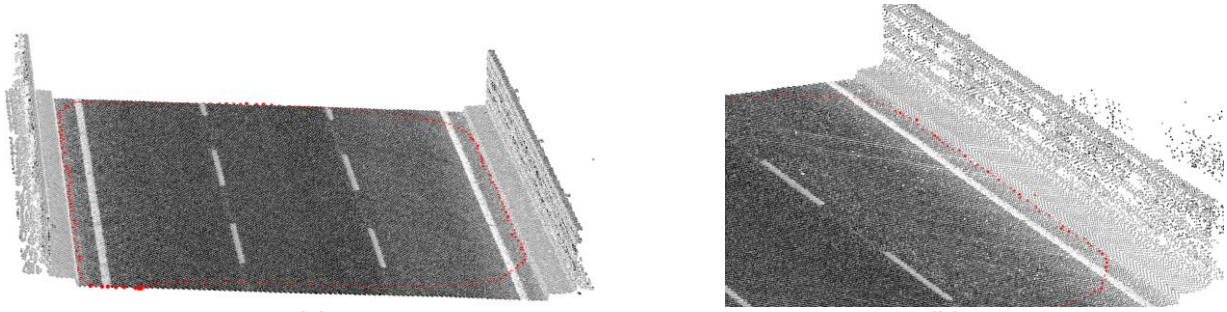

(a) (b)

Figure 8: (a) Planar view of estimated road edges over second road section highlighted in red colour (b) zoomed-in estimated road edges over second road section.

As seen from the results, the GVF snake model has performed qualitatively well. The snake contour converged along the edges of the road sections by utilizing the derived energy functions from LiDAR point cloud data. Results along the right edge were less accurate due to lower density of points on the right edge of the road than the left edge because of the use of a single laser scanner in our MMS. The initialisation of the snake contour using the navigation data has shown good results and was performed completely automatically. The weight parameters provided to the snake contour were manually adjusted. We intend to investigate

whether a correlation exists between the weight parameters and the input data in order to automate the process. We have tested the snake algorithm over small road but we intend to expand our tests to larger sections through batch-processing of LiDAR point cloud datasets.

6. CONCLUSION

We presented a method for extracting the road edges from the LiDAR and navigation data using the GVF snake model. The edge extraction results have been quite promising in terms of initialisation and in deriving the external energy terms by utilizing the capabilities of navigation and LiDAR data. The snake contour was initialized based on the heading and trajectory information provided by the navigation subsystem of the mobile van while the GVF and external energies were derived from the LiDAR point cloud attributes. The slope values and intensity pulse information can be utilized to differentiate the road surfaces from other features, thus deriving the energy functions from this information provided the snake contour to converge along the road edges. The presented method has been tested over the curb-side road sections where the difference between the slope values of curbs and planar road surface is significant. Future work would be focused over the non curb-side road sections and over investigating the best approach to qualitatively test the accuracy of our algorithm.

ACKNOWLEDGEMENTS

The authors would like to acknowledge the support received from the Irish Research Council for Science, Engineering and Technology (IRCSET) and Enterprise Partner Pavement Management Systems Ltd.

REFERENCES:

Amini, A.A., Weymouthm, T.E. & Jain, R.C., 1990. Using dynamic programming for solving variational problems in vision. *IEEE Transactions on Pattern Analysis and Machine Intelligence*, 12(9), 855-867.

Clode, S., Kootsookos, P. & Rottensteiner, F., 2004. The automatic extraction of roads from lidar data. In *International Archives of Photogrammetry, Remote Sensing and Spatial Information Sciences, Vol. XXXV, Part B3*.

Cohen, L., 1991. On Active Contour Models and Balloons. *CVGIP: Image Understanding*, 53(2), 211-218.

ERA-NET, 2009. Safety at the Heart of Road Design. , (February), 1-10. Available at: http://www.eranetroad.org/.

ERSO, 2008. Annual Statistics Report 2008: ERSO. *Transport*, 1-64. Available at: http://www.erso.eu.

Eenink, R, Reurings, M, Elvik, Cardoso, J, Wichert, S, Stefan, C., 2008. Accident Prediction Models and Road Safety Impact Assessment: recommendations for using these tools. *RIPCORD*, 1-20. Available at: http://ec.europa.eu.

European Commission, E.A., 2006. Road Transport Policy. , 1-16. Available at: http://ec.europa.eu/transport/road_safety.

Gatti, G. et al., 2007. Safety Handbook for Secondary Roads. *RIPCORD*, (January 2005), 1-227. Available at: http://ec.europa.eu.

Goepfert, J. & Rottensteiner, F., 2009. Adaption of Roads to ALS data by means of network snakes. In *International Archives of Photogrammetry, Remote Sensing and Spatial Information, Part3/W8*. Paris, France, pp. 24-29.

Hu, X., Tao, C.V. & Hu, Y., 2004. Automatic road extraction from dense urban area by integrated processing of high resolution imagery and lidar data. In *International Archives of Photogrammetry, Remote Sensing and Spatial Information Sciences, Vol. XXXV, Part B3*. Istanbul, Turkey.

Hunter, G., Cox, C. & Kremer, J., 2006. Development of a commercial laser scanning mobile mapping system - STREETMAPPER. In *Proceedings of Second International Workshop on the Future of Remote Sensing*. Antwerp, Belgium.

Kabolizade, M., Ebadi, H. & Ahmadi, S., 2010. An improved snake model for automatic extraction of buildings from urban aerial images and LiDAR data. *Computers, Environment and Urban Systems*, 1-7.

Kass, M., Witkin, A. & Terzopoulos, D., 1988. Snakes: Active Contour Models. *International Journal of Computer Vision*, 1(4), 321-331.

Kerschner, M., 2001. Homologous twin snakes integrated in a bundle block adjustment. *ISPRS Journal of Photogrammetry and Remote Sensing*, 56(1), 53-64.

Kingston, T. et al., 2007. An integrated mobile mapping system for data acquisition and automated asset extraction. In *5th International Symposium on Mobile Mapping Technology (MMT'07)*. Padua, Italy, pp. 1-5.

Leroy, B., Herlin, I. & Cohen, L., 1996. Multi-resolution algorithms for active contour models. In *International Conference on Analysis and Optimization of Systems Images ICAOS'96*. Paris, France, pp. 58-65.

Novak, K., 1993. New Tools for the Fast Collection of GIS Information. *Proceedings of SPIE*, 1943, 188-198.

Saeedi, S., Samadzadegan, F. & El-sheimy, N., 2009. Object extraction from lidar data using an artificial swarm bee colony clustering algorithm. In *International Archives of Photogrammetry, Remote Sensing and Spatial Information Sciences, Vol. XXXVIII, Part 3/W4*. Paris, France, pp. 133-138.

SafetyNet, 2009. Road Safety Management. , 1-41. Available at: http://ec.europa.eu/transport.

Tao, C.V. & Li, J., 2007. *Advances in Mobile Mapping Technology*, London: Taylor and Francis.

Vosselman, G. & Liang, Z., 2009. Detection of curbstones in airborne laser scanning data. In *International Archives of Photogrammetry, Remote Sensing and Spatial Information Sciences, Vol. XXXVIII, Part 3/W8*. Paris, France.

Xu, C. & Prince, J.L., 1998. Snakes, shapes, and gradient vector flow. *IEEE transactions on image processing*, 7(3), 359-69.

Yuan, X., Zhao, C. & Chen, D., 2008. Road-surface Abstraction using Ladar Sensing. In *IEEE International Conference on Control, Automation, Robotics and Vision*. Hanoi, Vietnam, pp. 1097-1102.